Polymer Degradation and Stability 183 (2021) 109388

Contents lists available at ScienceDirect

Polymer Degradation and Stability

journal homepage: www.elsevier.com/locate/polymdegradstab

Mass spectrometry investigation into the oxidative degradation of poly(ethylene glycol)

Molly E. Payne[a], Oluwapelumi O. Kareem[a], Kayla Williams-Pavlantos[b], Chrys Wesdemiotis[b], Scott M. Grayson[a,*]

[a] Department of Chemistry, Tulane University, New Orleans, LA 70118, United States
[b] Department of Chemistry, The University of Akron, Akron, OH 44325, United States

ARTICLE INFO

Article history:
Received 29 May 2020
Accepted 6 October 2020
Available online 9 October 2020

Keywords:
Poly(ethylene glycol) (PEG)
Oxidative degradation
MALDI-TOF MS
ESI-MS^2

ABSTRACT

Poly(ethylene glycol) (PEG) is an inexpensive, commercially available polymer that has many biomedical and material applications. Due to its water-solubility and biocompatibility, it has been used in drug conjugation, as a humectant, as an anti-foaming agent in food, and as a stabilizer for preservation of antique wooden objects. Despite the robust applications of PEG, the products of oxidative degradation are not fully understood. Using matrix-assisted laser desorption ionization time-of-flight mass spectrometry (MALDI-TOF MS), the end groups of PEG oxidative degradation products can be proposed. Confirmation of the proposed end groups can be corroborated via selective functionalization reactions as well as electrospray ionization (ESI) tandem mass spectrometry (MS^2). Furthermore, the oxidative degradation mechanism of PEG is described here by examining the degradative products using these aforementioned techniques. These findings suggest consistent oxidative behavior for both narrowly dispersed and monodisperse PEG. However, examination of monodisperse PEG allowed for the elucidation of certain degradation behavior due to the presence of a single starting peak, rather than a distribution of peaks, as found in narrowly dispersed PEG. These results demonstrate that MALDI-TOF MS, ESI MS^2, and selective functionalization reactions can be applied to the elucidation of polymer end groups and aid in identifying degradation mechanisms.

1. Introduction

Poly(ethylene glycol) (PEG) is a hydrophilic polyether that is synthesized via a ring opening polymerization of ethylene oxide and is commercially available in a variety of molecular weights and architectures. This ubiquitous polymer is typically narrowly dispersed and used in a variety of commercial, industrial, and medical applications. For example, PEG can be found as a food additive, [1] an additive in cosmetics, [2] a drug carrier, [3–5] an electrolyte in energy storage devices, [6] and various other applications. With low toxicity and immunogenicity in humans, PEG is used in a variety of medical applications from improving drug persistence [3] to forming hydrogels for wound care. [7] PEG also functions as the active ingredient in an over-the-counter treatment of constipation by inducing osmotic diarrhea. [8–10] Due to the aqueous swelling behavior of PEG and its solubility in water, it has also been used both as a modern day wood preservative and for the conservation of dried wooden artifacts such as the Skuldelev Viking ships, the English Mary Rose, [11] and the Swedish warship Vasa. [12–16] By impregnating the waterlogged wood with an aqueous solution of PEG, the integrity of the wood is preserved by preventing common issues upon drying, such as distortion and cracking [13].

Despite the robust applications of PEG, it is a labile polymer that is susceptible to degradation with moderate heating, [17,18] oxidative conditions, [17,19] microbiological exposure, [20] and autooxidation.[21] PEG is regarded as a biocompatible and nontoxic polymer, but there has been concern about how reactive impurities, under these oxidative conditions, can be both toxic and lead to further degradation. [22,23] The degradation products of PEG have been the subject of many studies due to their impact on the environment, [24] health, [22] and material applications. [22] Goglev et al. [25] were of the first to elucidate the thermal-oxidative degradation products of PEG and propose a mechanism. They identified the predominant degradation products to be water and formaldehyde, the latter of which is a toxic and volatile substance. They proposed that these oxidative products were the result of the formation of a hydroperoxide key intermediate. Chen et al. [26] were able to identify the presence of hydroperoxide PEG using electron spin resonance (ESR) spin trapping and hypothesized that

* Corresponding author.
E-mail address: sgrayson@tulane.edu (S.M. Grayson).

https://doi.org/10.1016/j.polymdegradstab.2020.109388
0141-3910/

they contribute to the oxidation of PEG. Other studies [27–29] have focused on the determination of the non-volatile components using nuclear magnetic resonance spectroscopy (NMR) and proposed their own mechanism. There is conflicting literature on whether the oxidative degradation originates at the ether bonds and is a result of chain scission of the C–O and C–C bonds [25,30] rather than the alcohol end group. [17,31] Mortensen [14] utilized matrix-assisted laser desorption ionization time-of-flight mass spectrometry (MALDI-TOF MS) to identify a number of degradation peaks in the polymer distribution of the PEG extracted from the Vasa. While he was able to propose reasonable assignments, he concluded that more experiments should be done to elucidate these structures since some of the identified masses overlapped with that of possible salt clusters.

Although there are many polymer characterization techniques available, few can provide as useful information about polymer end group analysis as MALDI-TOF MS. When sample preparation and data acquisition parameters are optimized, spectra should be obtained with sufficient resolution and mass accuracy to enable determination of overall molecular weight distribution, repeat unit mass, and subsequently, end groups of most homopolymers. [32] However, unlike NMR and SEC, MS utilizes only a fraction (as little as 1 μg) of each sample. While MALDI-TOF MS allows for the mathematical determination of a logical end group, selective functionalization reactions can help confirm the proposed structure. In addition to selective functionalization reactions, ESI-tandem mass spectrometry (ESI-MS^2) can be applied to verify the proposed oxidative degradation products of PEG. In MS^2 analysis, one n-mer of the polymer is isolated as the parent ion. This parent ion is then excited via collisionally activated dissociation (CAD) and separates into unique fragments that correlate to the n-mer structure. Ions can undergo charge induced or charge-remote dissociations, the extent of which depends on the structure of the parent ion. Elucidation of the polymer connectivity and end groups is facilitated by the use of a universal nomenclature system which was introduced based on the fragmentation mechanisms of polymer ions [33].

In this work, a variety of analytical techniques including MALDI-TOF MS, ESI MS^2, gel permeation chromatography (GPC), and NMR were utilized to elucidate the non-volatile oxidative degradation products of PEG using hydrogen peroxide as the oxidant. While NMR and GPC are useful in characterizing the type of functional groups present and the change in dispersity, respectively, they do not give the same insight to end group analysis as MALDI-TOF MS. After reasonable structures were assigned to the peaks identified by MALDI-TOF MS and ESI MS^2 selective functionalization reactions were subsequently used to confirm the identity of the proposed structures. Both narrowly and monodisperse PEG were used to help elucidate the mechanism of oxidative degradation, but the monodisperse PEG was able to give some mechanistic insight due to the presence of one starting peak rather than a distribution.

2. Experimental section

2.1. Materials

Hydrogen peroxide solution (Sigma), hydrazine monohydrate (TCI), acetic anhydride (Sigma), valeric anhydride (Sigma), and 4-dimethylaminopyridine (Sigma) were all used without purification.

2.2. Degradation of narrowly disperse PEG

M_n = 2000 dihydroxy PEG (Sigma) was dried in a vacuum oven overnight at 50 °C. The peroxide solution was prepared by diluting 30% hydrogen peroxide solution (Sigma) to a final concentration of 4.9 M. The PEG and peroxide solution were added to a reaction flask equipped with a stir bar at a concentration of 100 mg polymer per 5 mL of solution. The flask was placed on a Schlenk line where it was put under vacuum and backfilled with nitrogen 3 times and finally left under inert atmosphere (N_2) to oxidize and shielded from light exposure. Aliquots were taken at various time points via a chloroform extraction [13] and characterized. MALDI-TOF MS were measured at 24, 48, 96, and 192 h (Fig. 1). The remaining product was worked up after 192 h to get the final product. ^{1}H NMR (Fig. S4) (300 MHz, $CDCl_3$): ∂ = 1.94 (br), **3.64 (br, PEG backbone),** 4.17 (s), 4.32 (t), 4.73 (s), 5.40 (s), 8.08 (s), 8.12 (s). ^{13}C NMR (Fig. S5) (75 MHz, $CDCl_3$): ∂ = 31.05, 61.86, 63.17, 67.03, 69.00, 70.44, **70.70 (PEG backbone),** 72.75, 111.15, 140.05, 161.10, and FTIR (Fig. S6): 1110 cm^{-1} (C–O, strong), 1710 cm^{-1} (C=O, medium), 2750 cm^{-1} (C–H stretch, strong), 3180–3660 cm^{-1} (O–H stretch, broad).

2.3. Degradation of monodisperse PEG-24

The PEG-24 was dried in a vacuum oven overnight at 50 °C (Fig. S2 ^{1}H NMR and S3 ^{13}C NMR). The peroxide solution was prepared by diluting 30% hydrogen peroxide solution (Sigma) to a final concentration of 4.9 M. The PEG and peroxide solution were added to a scintillation vial equipped with a stir bar at a concentration of 100 mg polymer per 5 mL of solution. The flask was placed on a Schlenk line where it was put under vacuum and backfilled with nitrogen 3 times and finally left under inert atmosphere to oxidize and shielded from light exposure. Aliquots were taken at various time points via a chloroform extraction [13] and characterized via MALDI-TOF MS (Figs. 8 and S7b).

2.4. Functionalization of monodisperse Me-(OCH_2CH_2)$_8$-OH and Me-(OCH_2CH_2)$_8$-CHO

The 8-mer of the monomethoxy monohydroxy PEG and the monomethoxy oxyacetaldehyde PEG were purchased from BroadPharm. These were functionalized with hydrazine to determine the extent to which the methoxy PEG aldehyde converted into the hydrazone and could no longer be observed by MALDI-TOF MS. The methoxy PEG alcohol, however, was still present and seen after reaction with hydrazine (Fig. S10).

2.5. Selective functionalization of carbonyl groups for 192-hour degraded PEG

Hydrazine monohydrate (TCI) was used to selectively functionalize carbonyl groups in the 192-hour degraded dihydroxy PEG. PEG (50 mg) was dissolved in 1 mL of methanol where 4 equivalents of hydrazine monohydrate were subsequently added. The reaction was run for 4 h and was precipitated into cold diethyl ether (DEE) and characterized by MALDI-TOF MS (Fig. 3). ^{1}H NMR (Fig. S8) (300 MHz, $CDCl_3$): ∂ =1.87 (br), 2.77 (br), **3.53 (br, PEG backbone),** 4.63 (s), ^{13}C NMR (Fig. S9) (75 MHz, $CDCl_3$): ∂ = 61.86, 67.04, **70.71 (PEG backbone),** 72.75, 95.72, and FTIR (Fig. S6): 1110 cm^{-1} (C–O, strong), 1640–1690 cm^{-1} (C=N, medium), 2750 cm^{-1} (C–H stretch, strong), 3180–3660 cm^{-1} (O–H stretch, broad).

2.6. Selective functionalization of hydroxy groups

Acetic anhydride (Sigma) was used to selectively functionalize hydroxy groups in the 192-hour degraded dihydroxy PEG by adding 20 equivalents of acetic anhydride and 1.1 equivalents of 4-dimethylaminopyridine (Sigma) to the PEG in dichloromethane (DCM). The reaction was left to run overnight and was purified by precipitation into diethyl ether (DEE) and characterized by MALDI-TOF MS (Fig. 4). ^{1}H NMR (Fig. S11) (300 MHz, $CDCl_3$): ∂ = 1.91 (br), 2.07 (s), **3.63 (br, PEG backbone),** 4.21 (t), 4.31 (t), 4.73 (s), 8.01 (s), ^{13}C NMR (Fig. S12) (75 MHz, $CDCl_3$): ∂ = 21.09, 63.17,

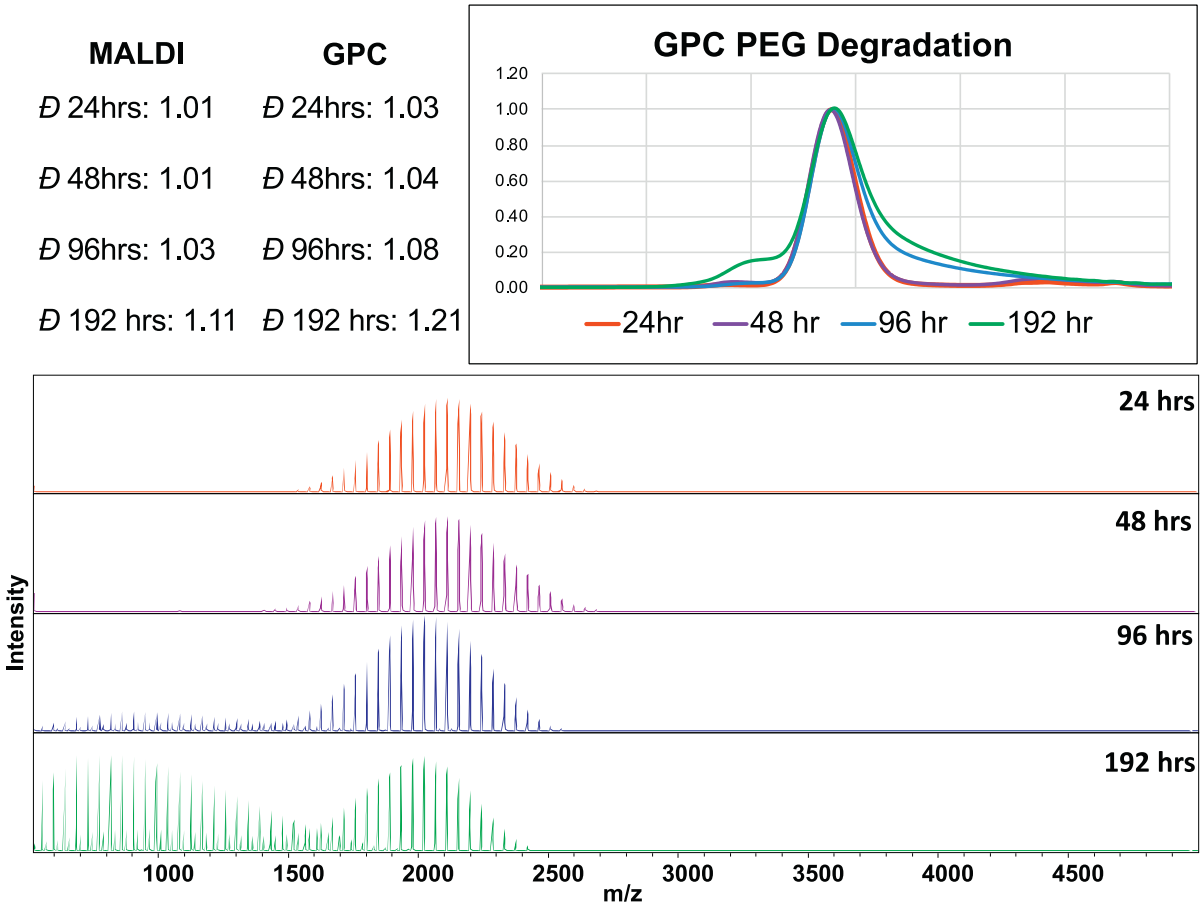

Fig. 1. MALDI-TOF MS and GPC spectra showing evolution of the degradation of PEG when exposed to 4.9 M H_2O_2 with aliquots taken at 24, 48, 96, and 192 h with their respective dispersity values.

63.73, 67.04, 69.00, 69.27, **70.71 (PEG backbone),** 95.72, 161.08, 171.14, and FTIR (Fig. S6): 1110 cm^{-1} (C–O, strong), 1710 cm^{-1} (C=O, medium), 2750 cm^{-1} (C–H stretch, strong), 3180–3660 cm^{-1} (O–H stretch, broad).

2.7. Characterization

A Bruker Autoflex III MALDI-TOF mass spectrometer (Bruker Daltonics, Billerica, MA) was used to collect Figs. 1–4, 7, and 8 as well as Figs. S1, S7, S10 and S13. Mass spectra data were collected in positive reflectron ion detection mode. Typical sample preparation for MALDI-TOF MS data was performed using 2 types of sample preparation. The first sample preparation was making stock solutions in tetrahydrofuran (THF) of matrix (20 mg/mL), polymer analyte (2 mg/mL), and a cation source (2 mg/mL). The stock solutions were combined in a 10/5/1 ratio (v/v) (matrix/analyte/cation) and plated via the dried droplet method. The second method was using graphite from a number 2 pencil as the matrix and subsequently plating 1 μL of polymer analyte solution and 1 μL of cation solution via the dried droplet method. Sodium trifluoroacetate (Sigma) was used as the cation source and *trans*-2-[3-(4-*tert*-butylphenyl)-2-methyl-2-propenylidene]malononitrile (DCTB) was used as the matrix in the first sample preparation. MALDI-TOF MS spectra were calibrated against SpheriCal dendritic calibrants (Polymer Factory, Sweden).

ESI-MS and ESI-MS^2 experiments (Figs. 5 and S14–S19) were carried out on a Waters Synapt HDMS quadrupole-time-of-flight (Q-ToF) mass spectrometer (Waters, Beverly, MA) equipped with an ESI source. For ESI-MS^2, stock solutions of the polymer and lithium trifluoroacetate (LiTFA) cationizing agent were prepared in MeOH at concentrations of 10 mg/mL for each. These solutions were then diluted in MeOH to 0.1 mg/mL (polymer) and 0.2 mg/mL (LiTFA) and mixed in a ratio of 2:1 (v/v) before being introduced into the ESI source via direct infusion at a flow rate of 20 μL/min. For ESI-MS, stock solutions were prepared in the same manner as that described above with the use of sodium trifluoroacetate (NaTFA) as the cationizing agent, as opposed to LiTFA. The instrument was operated in positive ion mode with a capillary voltage of 3.10 kV, an extraction cone voltage of 3.5 V, sampling cone voltage of 40 V, desolvation gas flow rate of 500 L/h (N_2), trap cell collision energy (CE) of 6.0 eV, transfer cell CE of 4.0 eV, trap gas flow of 1.5 mL/min (Ar), source temperature of 120 °C, and desolvation temperature of 250 °C. ESI-MS^2 experiments were carried out via collisionally activated dissociation (CAD) using Ar as collision gas in the trap cell with a collision energy of 40 eV (the transfer cell CE was set at 10.0 eV).

Gel permeation chromatography (GPC) was performed on a Waters Model 1515 isocratic pump and a Waters Model 2487 differential refractometer detector (Waters Corp., Milford, MA) with two columns in series PSS SDV analytical linear M (8 × 30 mm) and PSS SDV analytical 100 Å (8 × 30 mm); (Polymer Laboratories Inc., Amherst, MA). Data (Fig. 1) were collected in THF at a flow rate of 1 mL/min at 30 °C.

Nuclear magnetic resonance (NMR) spectroscopy was performed on a Bruker AVANCE 300 MHz spectrometer (Fig. 6, and Figs. S2–5, S8–9, S11–12). ^1H (300 MHz) and ^{13}C (75 MHz) experiments were performed at ambient probe temperate at a concentration of 10 mg/mL in chloroform-d ($CDCl_3$), purchased from Cam-

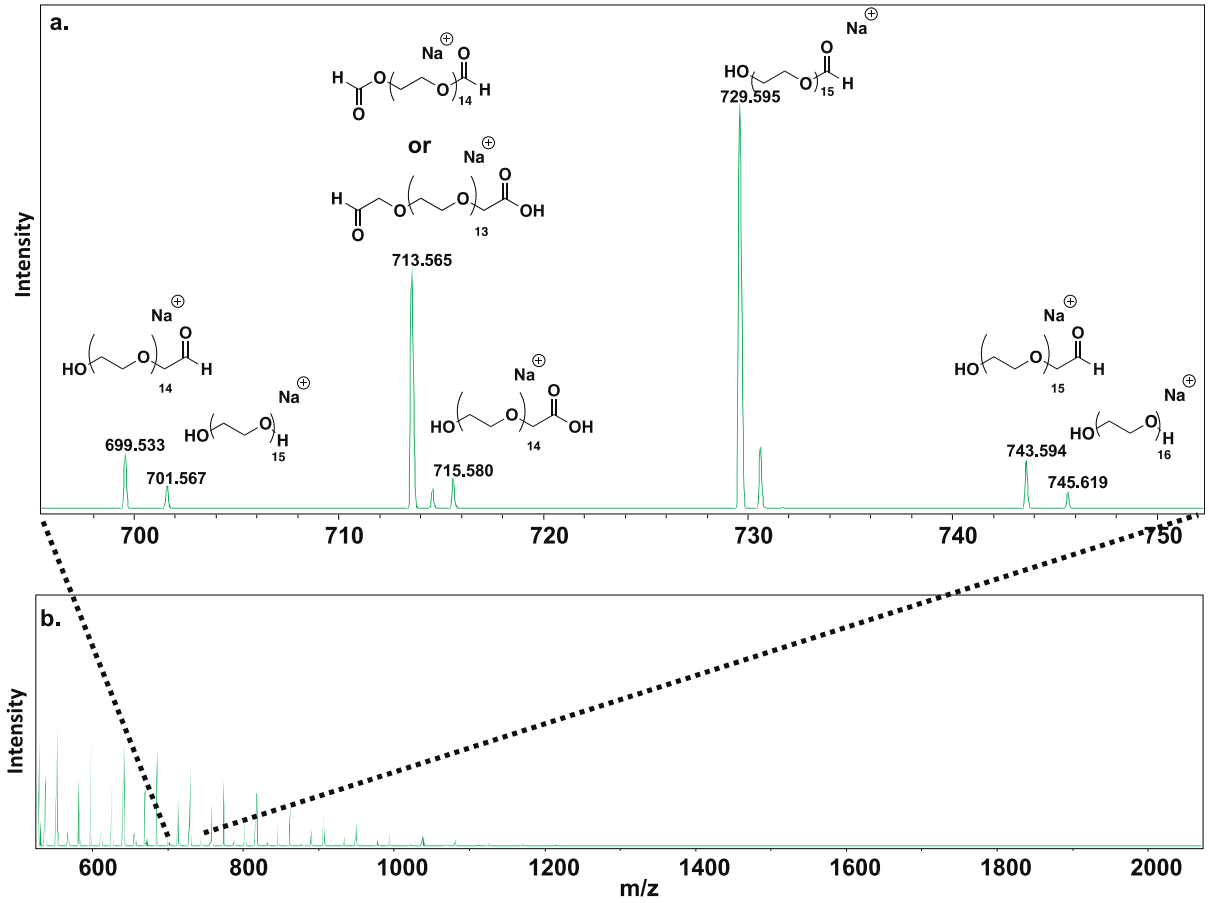

Fig. 2. (a). 700–750 region MALDI-TOF mass spectrum of a distribution of peaks from M_n = 2000 dihydroxy PEG after being exposed to 4.9 M H_2O_2 for 192 h. (b). Full MALDI-TOF mass spectrum of M_n = 2000 dihydroxy PEG after being exposed to 4.9 M H_2O_2 for 192 h.

bridge Isotope Laboratories (Andover, MA, USA). A sufficient number of scans were acquired to generate adequate signal to noise with a relaxation delay of 5 s.

Attenuated total reflection Fourier-transform infrared (ATR-FTIR) measurements were performed on a Nicolet iS50R spectrometer. Data (Fig. S6) were recorded at room temperature between 4000 cm^{-1} and 500 cm^{-1} at a resolution of 4 cm^{-1} and 32 scans were averaged for each spectrum.

3. Results and discussion

3.1. General degradation

While MALDI-TOF MS and ESI MS^2 were the focus of our characterization because of their ability to determine polymer end groups due to their resolution and mass accuracy, it was also important to compare the data obtained by MALDI-TOF MS to that from other analytical methods such as GPC. Fig. 1 shows that MALDI-TOF MS and GPC generally agree that degradation is occurring, though there is a difference in how much is occurring at each time point. Due to the mass ionization bias of MALDI-TOF MS (i.e. lower molecular weight ions have the potential to show a higher intensity of signal), the GPC analysis was important in understanding the changes in dispersity ($Đ$) of the oxidized PEG. The calculated $Đ$ is consistently higher by GPC with values of 1.03, 1.04, 1.08, and 1.21 for 24, 48, 96, and 192 h, respectively, when compared to MALDI-TOF MS with Đ values of 1.01, 1.01, 1.03, and 1.11. To determine degradation by MALDI-TOF MS, the integration under the PEG peaks before degradation was compared to the integration of any peaks formed during the degradation of PEG. When integrating the area under the MALDI-TOF MS peaks, it was found that at 24 h 0% was degraded, at 48 h 0.3% was degraded, at 96 h 6.0% was degraded, and at 192 h 61.2% was degraded. Though GPC is a qualitative technique, its dispersity and integration calculations are better for understanding molecular weight change during oxidative degradation. The low mass ionization bias of MALDI-TOF MS skews its calculated dispersity values and resulting degradation peak integrations. By integrating the GPC curve, there is 9.8% degradation at 24 h, 13.3% degradation at 48 h, 18.4% degradation at 96 h, and 46.1% degradation at 192 h.

Due to the potential of O_2 exposure during the aliquot process, a larger batch of PEG was degraded at the same concentration but left undisturbed for 192 h and subsequently extracted with chloroform and characterized via MALDI-TOF MS, GPC, ^1H NMR and ^{13}C NMR. While nothing was observed below 1200 Da in the starting material, a number of signals appeared between 500 and 1200 Da once degradation began. Fig. 2a shows oxidation after 192 h exposed to 4.9 M H_2O_2 for 700–750 Da from the overall distribution (Fig. 2b) to characterize the end groups. Peaks were observed at 699.53 Da, 701.57 Da, 713.57 Da, 715.58 Da, and 729.60 Da. The peaks at 743.59 Da and 745.62 Da correspond to an additional repeat unit in 699.53 Da and 701.57 Da, respectively. While reasonable assignments have been made for each of these peaks, their proposed identity will be addressed individually in the context of selective functionalizations, reasonable reaction mechanisms, and mass error when examined by tandem mass spectrometry (MS^2).

While having proposed logical structures that correspond to the identified masses, one of the only ways to prove what the end groups are on the degraded PEG is to use reagents that will selec-

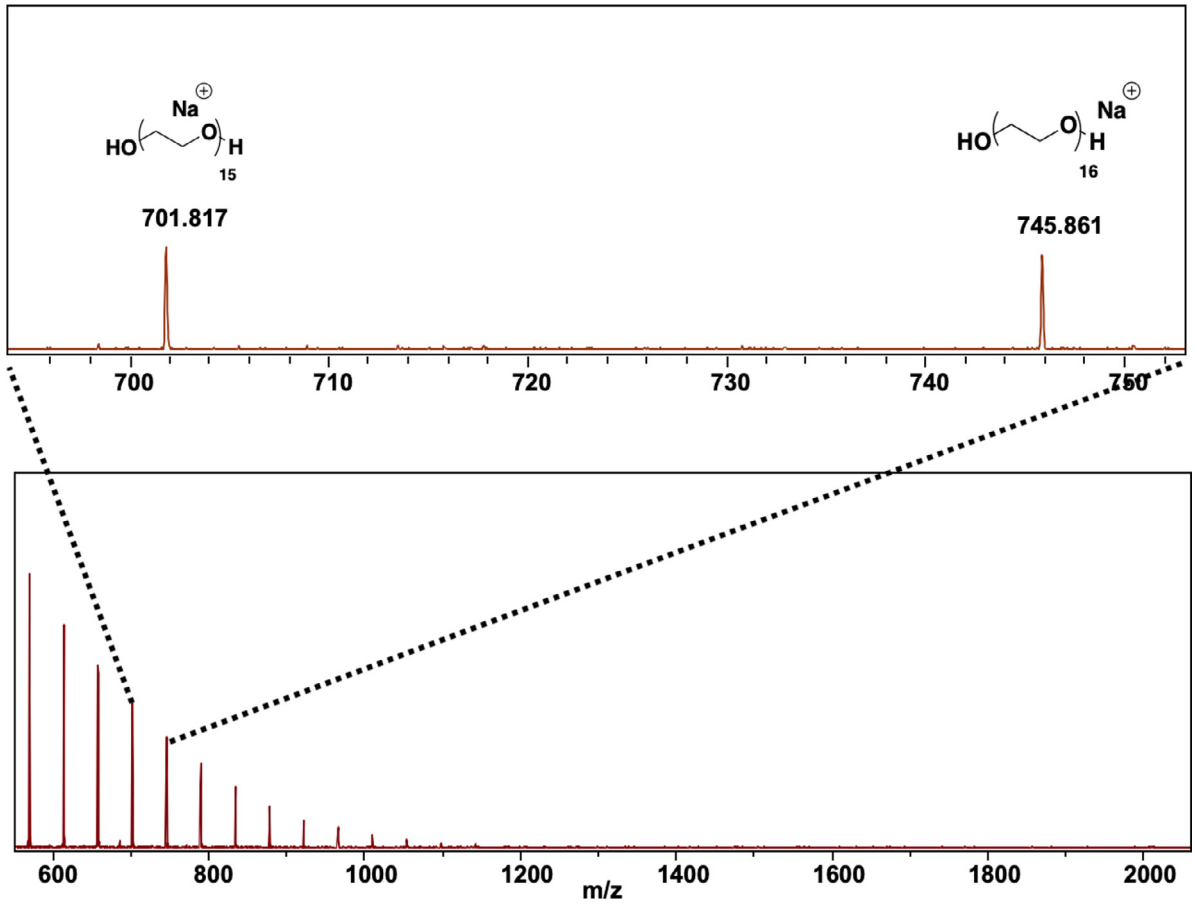

Fig. 3. MALDI-TOF mass spectra of the products of 192 h degraded PEG functionalized with hydrazine.

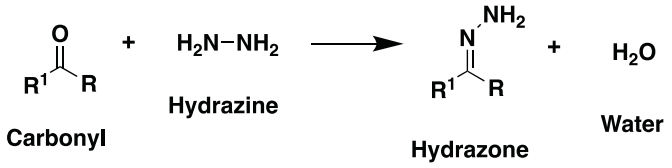

Scheme 1. Hydrazine selectively reacts with carbonyl functional groups to form a hydrazone.

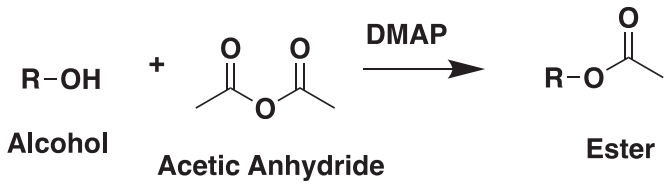

Scheme 2. Selective functionalization of an alcohol with acetic anhydride to form an ester.

tively functionalize each of the proposed end groups. In this case, hydrazine will selectively functionalize carbonyl groups (Scheme 1) while leaving hydroxy groups unreacted. Fig. 3 shows MALDI-TOF MS spectra for the hydrazine reaction with 192 h degraded PEG. When comparing the 192 h degraded PEG (Fig. 2) to the hydrazine functionalized PEG it is apparent that all of the proposed structures in the 192 h PEG that contain a carbonyl group were suppressed and the dihydroxy PEG peaks increased as a result. Using the monodisperse monomethoxy/oxyacetaldehyde PEG, the suppression of hydrazone containing groups were confirmed in the MALDI-TOF MS (Fig. S10).

An additional reaction with acetic anhydride was used to selectively functionalize structures that contain hydroxy groups to form an ester (Scheme 2). Fig. 4 shows the overall distribution, as well as low and high molecular weight insets of the functionalization (Table S1). When comparing the 192 h degraded PEG to the acetic anhydride functionalized 192 h PEG at 700 to 750 Da (Fig. 4), the majority of the peaks should shift since the majority of the proposed structures contain a hydroxy group or a carboxylic acid which can be coupled. The individual peaks as they related to the original 192 h degraded PEG (Fig. 2) are in the peak analysis section.

Finally, a reaction with valeric anhydride was used to selectively functionalize structures that contain hydroxy groups to form an ester (Scheme S1). Fig. S13 shows the overall distribution, as well as a low molecular weight inset of the functionalization. When comparing the 192 h degraded PEG to the valeric anhydride functionalized 192 h PEG at 700 to 750 Da (Fig. S13) the majority of the peaks should shift since the majority of the proposed structures contain a hydroxy group (Table S1). The individual peaks of the original 192 h degraded PEG (Fig. 2) and their post-functionalized variants are discussed below.

3.2. Peak 699.53 analysis

The peak at 699.53 Da (theoretical: 699.38 Da) (Fig. 2) corresponds to a mass that could account for one end of the 14-mer containing a hydroxy group and one group containing an oxyacetaldehyde. This also appears at 743.59 Da (theoretical: 743.40 Da) with the 15-mer when sodiated (ionized with sodium) (Table S1).

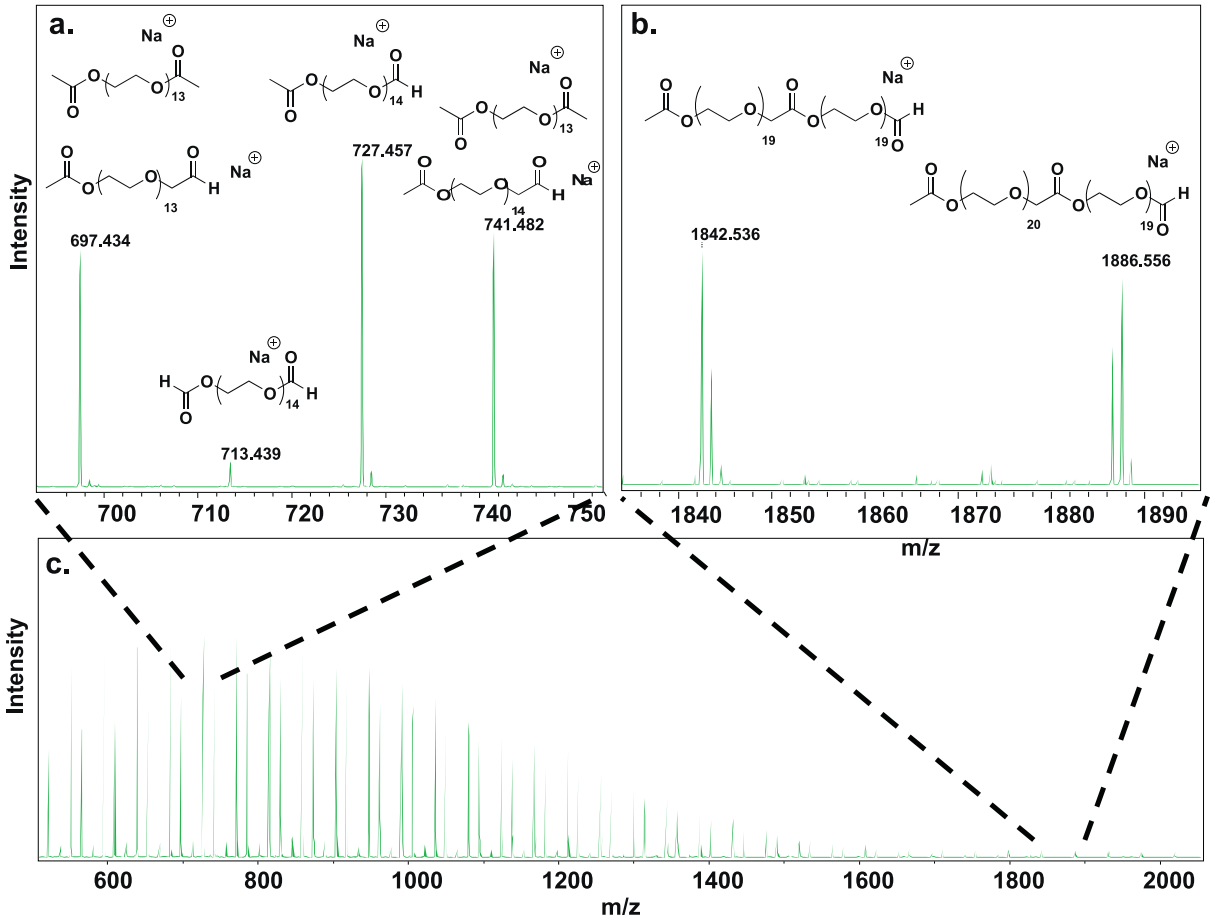

Fig. 4. MALDI-TOF mass spectra of 192 h degraded PEG reacted with acetic anhydride to selectively functionalize hydroxy groups.

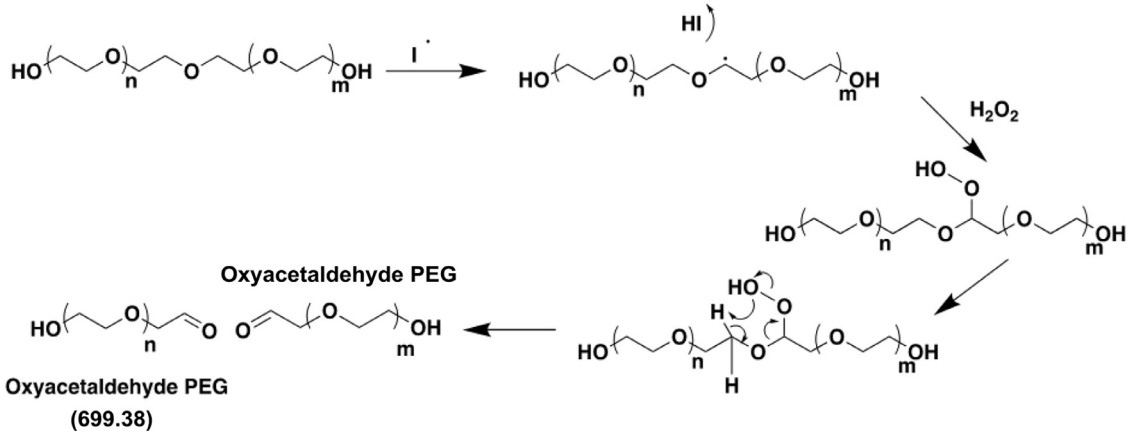

Scheme 3. Chain cleavage of PEG to yield oxyacetaldehyde products.

When a diol is oxidized, an aldehyde is a potential degradation product (Scheme 3) which is 2 Da less than the respective dihydroxy PEG peaks (701.57 Da in this case). Once functionalized with hydrazine to test if carbonyls were present (Fig. 3), this monooxyacetaldehyde monohydroxy 14-mer at 699.53 Da disappears due to the formation of a hydrazone. Hydrazones are shown to be ineffective at ionizing (Fig. S10). The presence of hydroxy groups was confirmed by the reaction with acetic anhydride (Fig. 4). Once functionalized with acetic anhydride, the 699.53 Da peak is shifted to 741.48 Da (theoretical: 741.39 Da). The 13-mer of the oxyacetaldehyde PEG (655.35 Da) with one acetate added (+42.01 Da) is also visible at 697.43 Da (theoretical: 697.36 Da). Unfortunately, this overlaps with the dihydroxy PEG when reacted with acetic anhydride to give the addition of two acetates at 697.43 Da (13-mer) and 741.48 Da (14-mer). However, in the valeric anhydride reaction (Fig. S13), the 12-mer and the 13-mer of the functionalized monoaldehyde PEG are seen at 695.69 Da (theoretical: 695.38 Da) and 739.69 Da (theoretical: 739.41 Da) respectively, which does not overlap with the valeric anhydride functionalized dihydroxy PEG of 693.75 Da (12-mer theoretical: 693.40 Da) and 737.77 Da (13-mer theoretical: 737.43 Da). The ESI-MS^2 fragmentation pattern (Fig. S14) is also in good agreement with the monooxyacetaldehyde

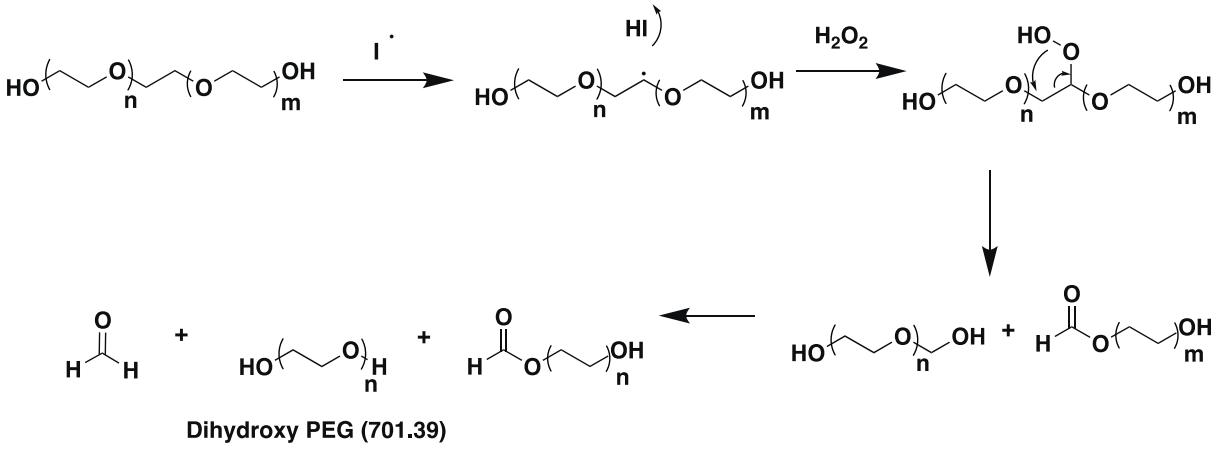

Scheme 4. Formation of dihydroxy PEG after oxidative degradation.

monohydroxy PEG structure ($(M+Li)^+$ = 595.35). The key "b" peak at 535.34 Da is indicative of the remaining PEG chain after a loss of the $HOCH_2CHO$ end group. The small mass error of 5.7 ppm (Fig. S16) calculated from the bulk spectrum (Fig. S15) also corroborates the proposed structure.

3.3. Peak at 701.57

The peak at 701.57 Da (theoretical: 701.39 Da) corresponds to the 15-mer of dihydroxy PEG when sodiated (Table S1). This is the result of polymer chain scission yielding a monoformate PEG and a hydroxymethyl group (hemiacetal). This hemiacetal is very unstable [27] and therefore not present in the mass spectrum. This hemiacetal quickly breaks down to form an alcohol (dihydroxy PEG) and formaldehyde (Scheme 4). Because this species does not contain any carbonyl groups, it will not functionalize with hydrazine (Fig. 3) and therefore does not form any hydrazone complexes. These hydrazone complexes ionize poorly by MALDI-TOF MS (Fig. S10) and therefore the intensity of the dihydroxy PEG increases. Because dihydroxy PEG contains two hydroxy groups, its 14-mer (657.37 Da) undergoes two functionalizations with acetic anhydride (+84.02 Da) and shifts to 741.48 Da (theoretical: 741.39 Da) (Fig. 4) when sodiated. Similarly to the functionalization with acetic anhydride, dihydroxy PEG also undergoes two functionalizations with valeric anhydride (+168.12 Da) (Fig. S13) for the 11-mer (525.29 Da) to shift to 693.75 Da (theoretical 693.40 Da) and the 12-mer (569.31 Da) to shift to 737.77 Da (theoretical 737.43 Da) when sodiated. The presence of dihydroxy PEG was also confirmed with MS^2 fragmentation patterns ($(M+Li)^+$ = 597.37) (Fig. S17) as well as a small mass error of 12.5 ppm (Fig. S16).

3.4. Peak at 713.57

The peak at 713.57 is perhaps the most complex in the distribution in that there is evidence to suggest that it is a diformyl ester PEG, a monooxyacetic acid monooxyacetaldehyde PEG, or perhaps both (Scheme 5). After functionalization with hydrazine to react with any carbonyls (Fig. 3), there is a complete lack of signal which confirms the formation of a hydrazone which would be the case for either the diformyl ester PEG or the monooxyacetic acid monooxyacetaldehyde PEG. The acetic anhydride functionalization proved plausible for both structures as well. While neither of the structures contain a hydroxy group, the monooxyacetic acid PEG can be coupled with acetic anhydride via DMAP to generate

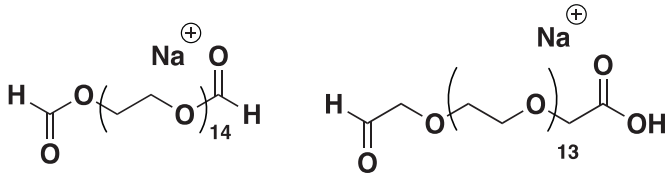

Scheme 5. Potential structures for the peak at 713.57 Da: diformate and oxyacetic acid /oxyacetaldehyde PEG.

the mixed acid anhydride. This would account for the high molecular weight peaks (Fig. 4b) of the spectrum such as 1842.54 Da when sodiated. This peak does not correspond to a higher molecular weight of any of the other proposed structures discussed, but actually corresponds to the coupling of the monooxyacetic acid monooxyacetaldehyde PEG coupling to the monoformyl PEG (theoretical: 1842.01 Da). Alternatively, 1842.54 Da could also be the monooxyacetic acid without the monooxyacetaldehyde PEG coupled to the monoformyl PEG and subsequently functionalized with acetic acid (theoretical: 1842.01 Da). After functionalization, there is a small peak at 713.44 Da which could correspond to the diformyl ester PEG not shifting due to the lack of a hydroxy or carboxylic acid functionality. This reduction in peak size compared to the original 192 h spectrum (Fig. 2) could potentially be due to hydrolysis of the formyl esters to monoformyl ester PEG and dihydroxy PEG. The spectrum of the valeric anhydride functionalization (Fig. S13) does not show any peaks that would correspond to the diformyl ester PEG or the monooxyacetic acid monooxyacetaldehyde PEG. This could be due to the hydrolysis of the diformyl ester PEG to either the monoformate or the dihydroxy PEG which would make sense based upon the large increase in the dihydroxy functionalized with valeric anhydride PEG peaks at 693.75 Da (11-mer) and 737.77 Da (12-mer).

Using MS^2, the fragmentation patterns (Fig. S18) are a better fit for the diformate rather than the monooxyacetic acid monooxyacetaldehyde PEG. Notably, from the starting material ($(M+Li)^+$ = 609.33 Da), the "c" fragment at 579.35 Da (12-mer with lithium) corresponds to the diformate PEG with the loss of a formaldehyde group (−30.01 Da) to yield an oxyacetaldehyde end group, and peak "b" at 563.33 which corresponds to the loss of a formic acid (−46.01 Da) while yielding the mass of a polymer with a vinyl ether end group. The mass error was calculated to be 32.3 ppm (Fig. S16) which is not unreasonable, but also is not definitive.

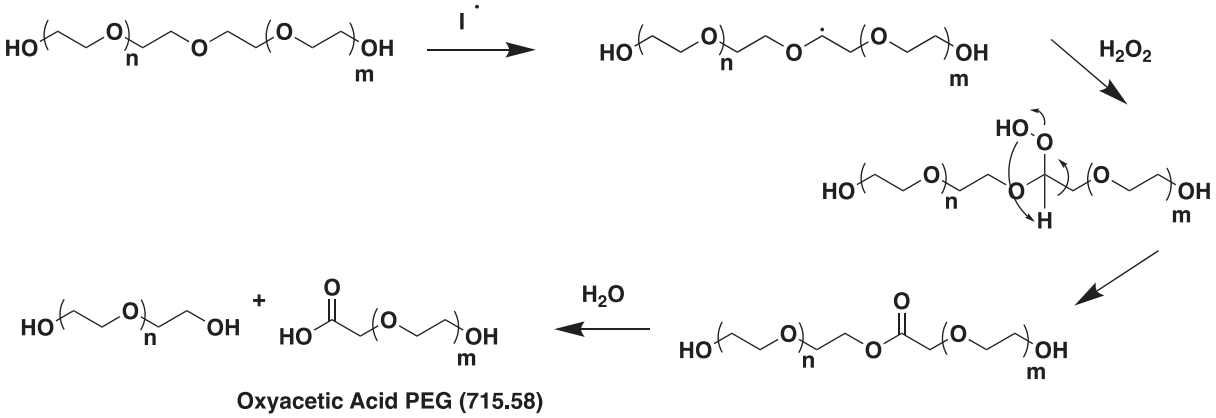

Scheme 6. Formation of monooxyacetic acid PEG.

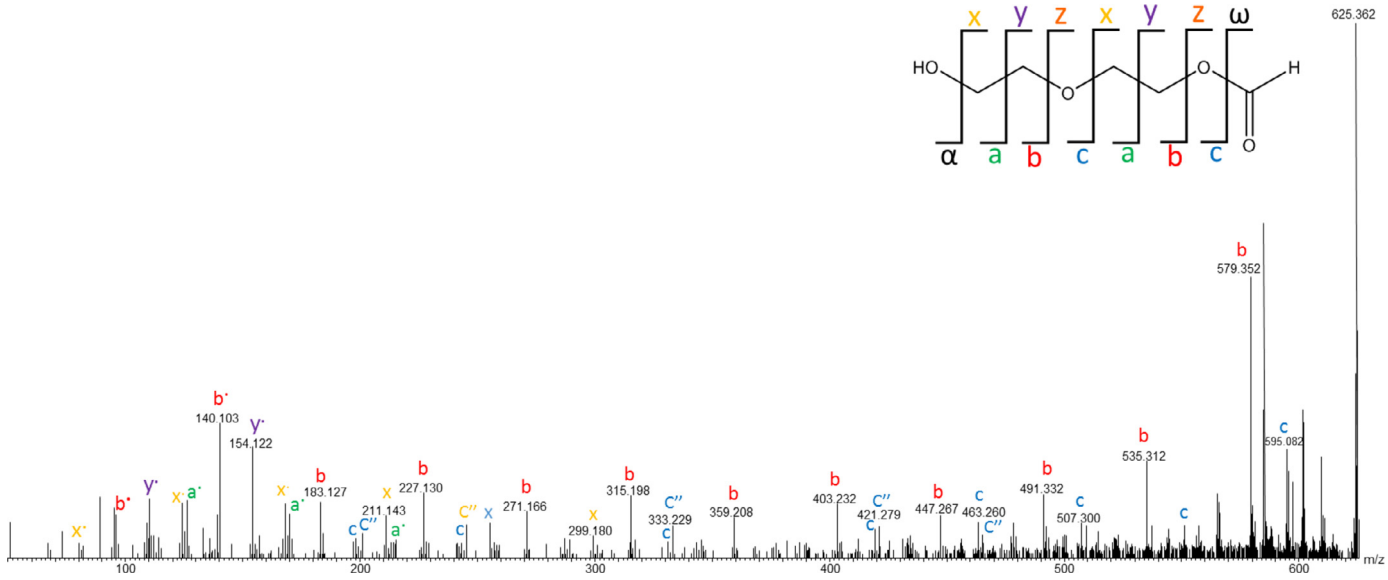

Fig. 5. ESI-MS^2 mass spectra of the lithiated 13-mer of monoformate terminated PEG (625.36 Da) which is analogous to the sodiated 15-mer of monoformate PEG (729.39 Da).

3.5. Peak at 715.58

The peak at 715.58 Da (theoretical: 715.37 Da) corresponds to a 14-mer PEG with an oxyacetic acid group on one end and a hydroxy group on the other end (Scheme 6). This is another potential oxidative degradation product of a PEG at its terminal alcohols. The carboxylic acid appears to react with hydrazine to form an acylhydrazine. With the formation of this poorly ionizing acylhydrazine as well as the hydrazone groups, only the dihydroxy PEG is observed in the spectrum of the hydrazine reaction product (Fig. 3). When functionalized with acetic anhydride (Fig. 4), a small amount of the 13-mer monoacetic acid is seen at 713.44 Da (theoretical: 713.36 Da) for a shift of plus one acetate group (+42.01 Da) to the monohydroxy compound (671.35 Da). Due to the presence of the oxyacetic group, it also potentially couples as an ester with the predominate byproduct, the monoformyl 25-mer (e.g. + 1146.66 Da), subtracting water (−18.01 Da), resulting in the peak at 1842.54 Da (theoretical: 1842.01 Da). We can confirm that this is in fact a carboxylic acid and not an in-chain ester because upon functionalization with acetic anhydride there should have been a peak at ~755.34 Da corresponding to two functionalizations with acetic anhydride if there were hydroxy groups on both ends. However, there was one (713.44 Da), but not two (~755.34 Da). For the valeric anhydride functionalization (Fig. S13), we see a peak at 711.76 Da (theoretical: 711.38 Da) which corresponds to the reaction of the 12-mer (627.32 Da) monohydroxy end group with one equivalent of valeric anhydride, but not on the carboxylic acid end. Using MS^2, the fragmentation pattern (Fig. S19) is a good fit to the monocarboxylic acid structure ($(M+Li)^+$ = 611.35). Notably, the peak "c" at 551.32 *m/z* corresponds to the lithiated 12-mer of the monooxyacetic acid PEG with the loss of acetic acid. The mass error was calculated (Fig. S16) from the bulk spectrum (Fig. S15) to be 17.7 ppm.

3.6. Peak at 729.60

It is important to describe the most intense peak which is the formyl ester at 729.60 Da (theoretical: 729.39 Da) which corresponds to the 15-mer with a hydroxy group on one end and a formyl ester on the other end (Table S1). For the majority of the degradation spectra by MALDI-TOF MS (48–192 h), this appears to be the most significant peak of all of degradation products. One reaction that had been proposed by Mortensen was if the hydroperoxide attacked at the beta carbon from either end group, the activated compound could be broken down to the polymer formyl peak and formaldehyde. This would only result in high molecular weight products (1500–2500 Da) since it happens at the end of the polymer chain. However, the degradation products are ap-

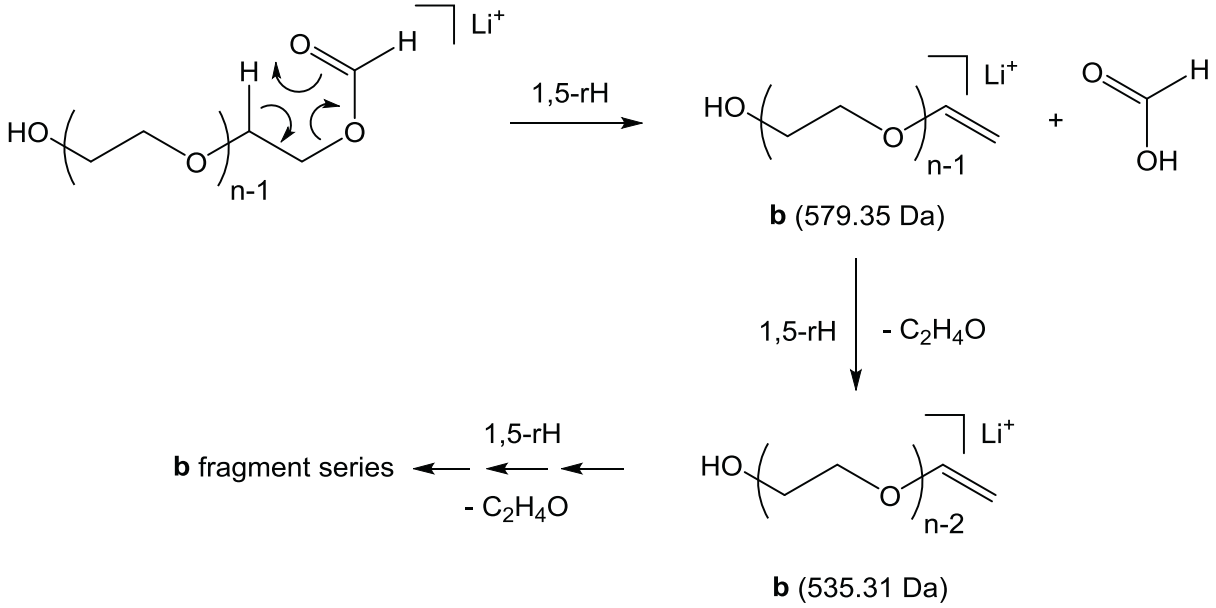

Scheme 7. PEG with Li^+ adducts can undergo charge-remote 1,5-H rearrangement (1,5-rH) at the formate group that leads to loss of formic acid and the formation of the b fragment ion at 579.35 Da with hydroxy and vinyl chain ends. Consecutive monomer losses via the same 1,5-rH mechanism lead to the dominant **b** fragment series. Competitive charge-remote homolytic C–O bond cleavages and charge-induced heterolytic C–O bond cleavages form the other, minor fragment series observed (adapted).[33].

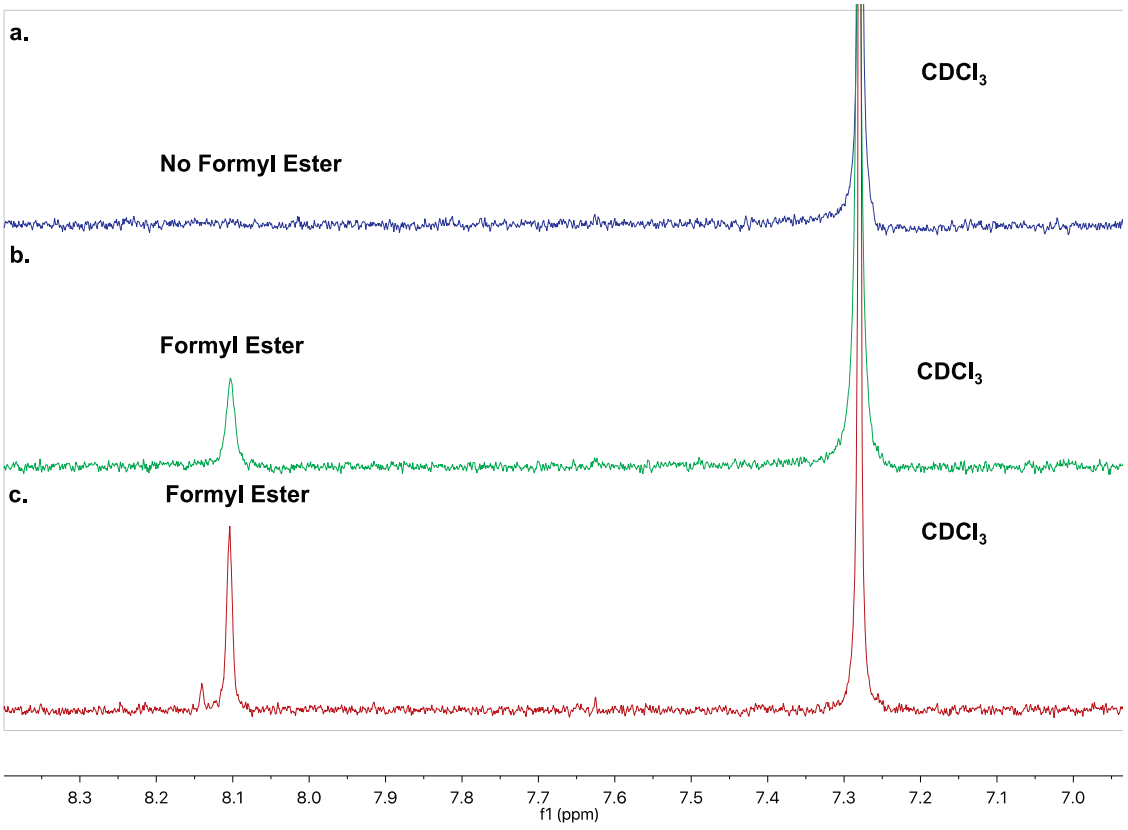

Fig. 6. ^1H NMR of the formyl region of the: (a). hydrazine functionalized 192 h degraded PEG, (b). acetic anhydride functionalized 192 h degraded PEG, and (c). 192 h degraded PEG.

proximately half the molecular weight of the starting material. This means that the degradation resulting in the formyl ester end group at approximately 700–1200 Da is caused by cutting each PEG chain approximately in half (Scheme 4). In this case, the remainder of the degradation is a hemiacetal group (which is not seen) on one half, and the hydroxy group on the other side of the chain. This hemiacetal end group rapidly degrades to form formaldehyde and the dihydroxy PEG.[14,27] When functionalized with hydrazine, the formate group is converted to a hydrazone and therefore will not ionize well for MALDI-TOF MS (Fig. S10). When acetic anhydride is reacted with the formyl ester PEG, the one hydroxy end group of the 14-mer is functionalized with an acetate and gives 727.48 Da

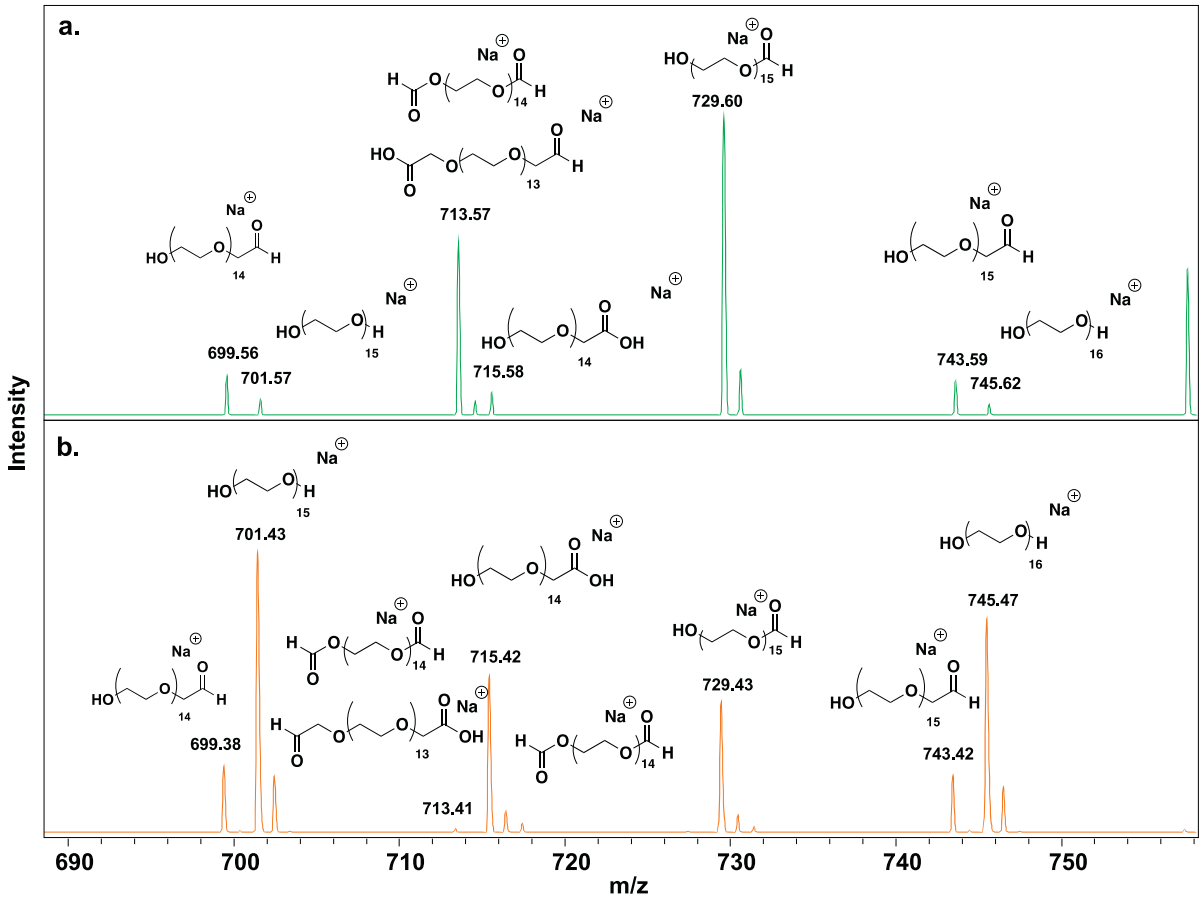

Fig. 7. MALDI-TOF mass spectra of (a). 192 h degraded M_n = 2000 Da dihydroxy PEG from 700 to 750 Da compared to (b). 192 h degraded PEG-24 (bottom) from 700 to 750 Da.

(theoretical: 727.37 Da) when sodiated. There is also potential for the monoformyl PEG (25-mer) to couple with monooxyacetic acid (13-mer) to create an ester plus one acetoxy group (+42.01 Da) and form the peak at 1842.54 Da (theoretical: 1842.01 Da). In the functionalization of the monoformyl ester with valeric anhydride (Fig. S13), there is a peak at 725.70 Da (theoretical: 725.39 Da) which corresponds to the 13-mer of the formyl ester functionalized with valeric anhydride. The low mass error of 3.9 ppm (Fig. S16) calculated from the bulk spectrum (Fig. S15) (Fig. 5) supports the proposed monoformate structure ($(M+Li)^+$ = 625.36) in the MS^2 fragmentation pattern when lithiated.

PEG and its degradation products can easily be ionized via adduct formation with alkali metal ions due to the oxygen-rich nature of the polymer.[33] Fig. 5 provides an ESI-MS^2 mass spectra of the lithiated 192 h degraded formate ester of PEG at 625.36. The presence of a formate end group is verified by the high intensity b_n fragment (579.352 Da), as a result of the degradation product undergoing the characteristic McLafferty rearrangement. As shown in Scheme 7, PEG with Li^+ adducts can undergo a charge-induced fragmentation at the CH_2–O bond that leads to the formation of fragments containing a hydroxy and formate end group (z_n" series) or a hydroxy and a vinyl end group (b_n series). This reaction proceeds via charge-induced heterolytic C–O bond cleavage, followed by hydride and proton transfers to produce both the z_n" and b_n fragments. The same mechanism can occur between the O–CH_2 bond, to produce the c_n" series (dihydroxy end groups) and the x_n series (vinyl and formate end group). In addition to the above mentioned fragmentation mechanism, homolytic cleavage of the polymer backbone leads to free radical intermediates, such as those shown in the low molecular weight region (b·, x·, c·, a·, and y·). The b·, x·, and c·, radical ions can then undergo beta hydride scission to form the b_n, x_n and c_n fragments (aldehyde and hydroxy end group). Additionally, the a· and y· radical ions can undergo beta methoxy scission followed by beta hydride scission to produce the b_n and x_n fragments respectively. These series are seen in the highest abundance in Fig. 5, as a result of charge induced mechanisms favoring small oligomers such as the degradation products discussed herein.

While MS techniques were able to identify aldehydes, carboxylic acids, and formates, NMR was only able to detect the presence of formates. Typically, polymer end group analysis by NMR is difficult because of the relatively large intensity of polymer backbone signals. However, due to the formation of formates as a major component of the product from oxidation, this region can be used to determine the success of functionalization (Fig. 6). A peak in the formate region (~8.1 ppm) is visible for the 192 h degraded PEG (Fig. 6c) and the acetic anhydride functionalized PEG (Figs. 6b). While in the 192 h degraded PEG reacted with hydrazine (Fig. 6a), this peak is absent due to the formation of a hydrazone functional group which forms an insoluble precipitant. Fig. 6c also shows the formic acid which is a byproduct of the degradation of the formate group, yielding a new dihydroxy PEG. This is also apparent in the ^{13}C NMRs of the 192 h degraded PEG (Fig. S5) which shows a substantial peak at 161.1 ppm which is the formate. The acetic anhydride functionalized (Fig. S12) PEG shows this peak (161.1 ppm) plus two additional peaks, the acetic ester at 171.1 ppm as well as the methyl at 21.1 ppm. The hydrazine functionalized (Fig. S9) does not show this peak at 161.1 or anything above 100 ppm demon-

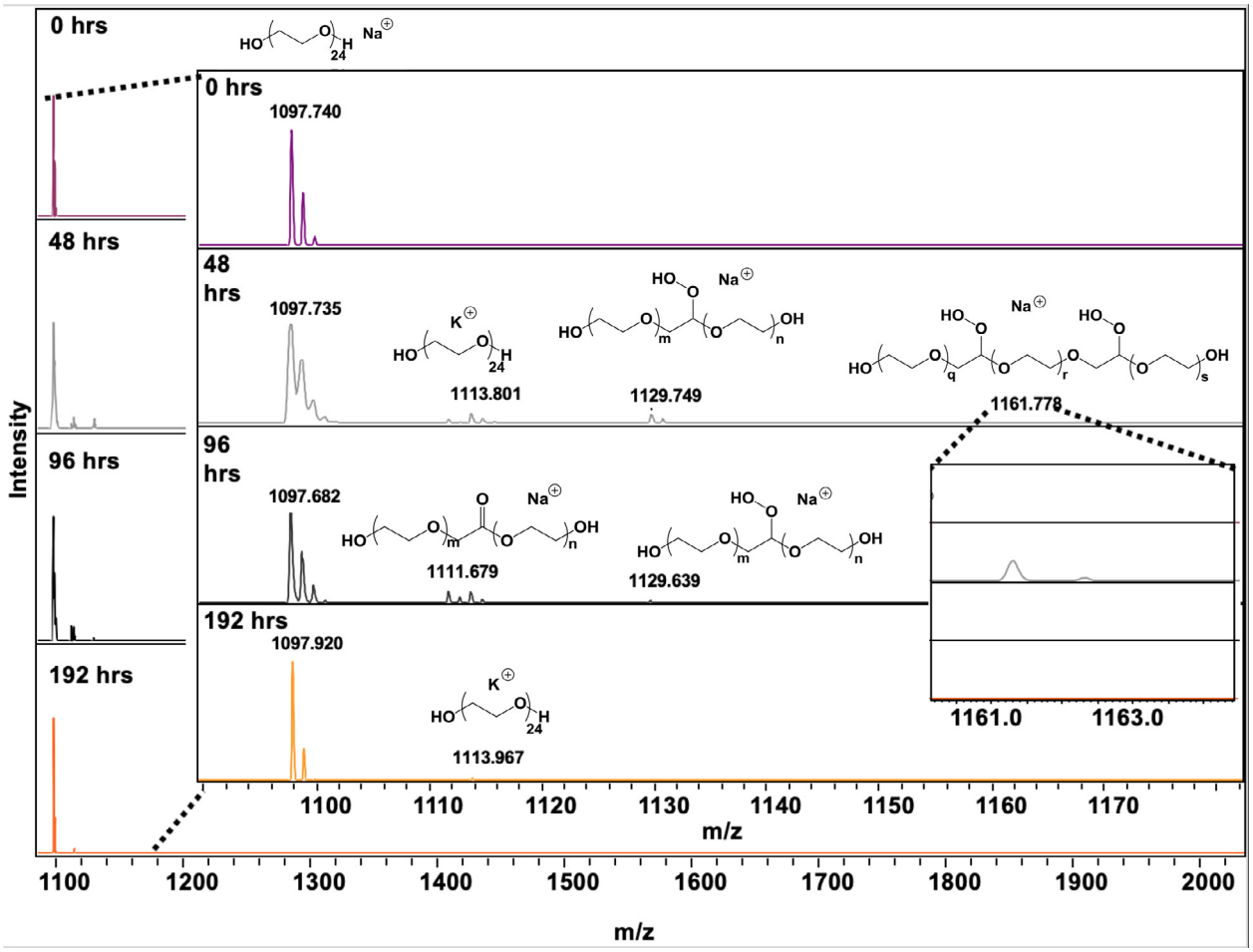

Fig. 8. MALDI-TOF mass spectra of 192 h degraded PEG-24 at 0, 48, 96, and 192 h shows formation of the dihydroperoxide and hydroperoxide at 48 h and hydroperoxide at 96 h with $n + m = 23$ and $q + r + s = 22$.

strating the complete functionalization of carbonyl groups with hydrazine. Finally, the FTIR (Fig. S6) shows the carbonyl peak at 1730 cm^{-1} is present in both the acetate functionalized PEG as well as the 192 hdegraded PEG. It is increased due to the amount of carbonyls from the residual formyl peaks, plus the acetate functionalization. This carbonyl peak is quenched in the hydrazine functionalized PEG, where the formation of the hydrazone peak at 1620–1690 cm^{-1} is indicative of the presence of the C=N resonance.

3.7. Monodisperse PEG-24

PEG is typically found as a narrowly dispersed polymer, but individual repeat units can be isolated via HPLC to yield a monodisperse polymer. By degrading a monodisperse polymer, the actual products of degradation, as well as the mode of degradation, become more apparent due to the lack of overlapping signals in the starting material of narrowly disperse PEG**.** The MALDI-TOF MS spectra show the 192 h degraded narrowly disperse PEG (Fig. S7a) and 192 h degraded monodisperse PEG (Fig. S7b). When comparing the degraded monodisperse PEG-24 to the 192 h degraded narrowly dispersed PEG (Fig. S7), it is apparent that cleavage of the polymer does not happen at one particular site (i.e. the end, the middle, etc.) and can be attributed to random chain scission. When looking at the products of degradation from the narrowly dispersed PEG and the monodisperse PEG-24 (Fig. 7), there are no new products in the degraded PEG-24. It is apparent that there are some potassium and sodium adducts, which are to be expected when using graphite as a matrix.

The most interesting aspect of the monodisperse PEG in the study of oxidative degradation is the ability to see the addition of a hydroperoxide via MALDI-TOF MS. Due to the overlapping peaks in a narrowly dispersed PEG, this is not readily visible. Fig. 8 shows the evolution of oxidation of PEG-24 over a 192 h time period with both a sodiated dihydroperoxide and hydroperoxide visible at 1161.78 Da and 1129.75 Da respectively, at 48 h, the formation of a hydroperoxide and an ester derivative at 96 h, and finally only a potassium adduct at 192 h. Between the 96 h period (with an ester at 1161.78 Da) and the 192 h period (without an ester), it appears that the majority of these break apart via hydrolysis to create a lower mass carboxylic acid (715.37 Da) and lower mass PEG diol. Seeing the addition of the hydroperoxide via mass spectrometry is especially interesting because it supports previously proposed reaction mechanisms which suggest the formation of a hydroperoxide intermediate [25,28,29,34]

4. Conclusions

In this study of the oxidative degradation of PEG, we have utilized various analytical techniques such as GPC, NMR, MALDI-TOF MS, and ESI-MS^2. MALDI-TOF MS is unique in its ability to determine repeat unit mass, and subsequently, the end groups of most homopolymers. While MALDI-TOF MS has been previously utilized in studying the degradation of PEG, [14] it has only been used to suggest structures that could potentially match the observed masses in a MALDI-TOF MS spectrum. For the first time, we not only propose structures, but also confirm their existence by selec-

tive functionalization reactions and corroborate that with ESI-MS^2 data. While many studies have done significant work with narrowly dispersed PEG or small oligomers [18,28,29,35,36] such as tetraethylene glycol, [17] this work demonstrates the usefulness of larger monodisperse PEGs in the understanding of the degradation mechanism by identifying hydroperoxides via mass spectrometry.

Author contributions

The manuscript was written through contributions of all authors. All authors have given approval to the final version of the manuscript.

Authorship contribution statement

Molly E. Payne: (MALDI-TOF MS, NMR, GPC, ATR-FTIR) Investigation, Data curation, Writing - original draft, Writing – review & editing; **Oluwapelumi O. Kareem:** (MALDI-TOF MS, NMR, GPC, ATR-FTIR)

Writing – review & editing; **Kayla Williams-Pavlantos:** (ESI-MS^2) Investigation, Data curation, Writing – review & editing; **Chris Wesdemiotis:** (ESI-MS^2) Supervision, Project administration, Writing – review & editing; **Scott Grayson:** (MALDI-TOF MS, NMR, GPC, ATR-FTIR) Conceptualization, Methodology, Supervision, Project administration, Writing - review & editing.

Declaration of Competing Interest

The authors declare that they have no known competing financial interests or personal relationships that could have appeared to influence the work reported in this paper.

Acknowledgments

The authors acknowledge Tulane University, the Louisiana Board of Regents for a graduate fellowship (M. E. P.), the Southern Regional Educational Board/Louisiana Board of Regents for a graduate fellowship (O. O. K.) and support from the Smart MATerials Design, Analysis, and Processing consortium (SMATDAP) funded by the National Science Foundation under the cooperative agreement IIA-1430280 is gratefully acknowledged. The experiments at the University of Akron were supported by a grant from the National Science Foundation (CHE-1808115). The authors also acknowledge the LA BOR RCS One year: LEQSF 2018-2019 RD-A-18 and Carol Lavin Bernick Faculty Grant. The monodisperse benzyl-PEG-24 was donated by Polypure AS, Oslo, Norway.

Supplementary materials

Supplementary material associated with this article can be found, in the online version, at doi:10.1016/j.polymdegradstab.2020.109388.

Appendix A: supplementary information

The following is the supplementary information to this article (See SI)

References

[1] M. Younes, P. Aggett, F. Aguilar, R. Crebelli, B. Dusemund, M. Filipič, M.J. Frutos, P. Galtier, D. Gott, U. Gundert-Remy, G.G. Kuhnle, C. Lambré, I.T. Lillegaard, P. Moldeus, A. Mortensen, A. Oskarsson, I. Stankovic, I. Waalkens-Berendsen, R.A. Woutersen, M. Wright, P. Boon, O. Lindtner, C. Tlustos, A. Tard, J.-C. Leblanc, EFSA panel on food additives and nutrient sources added to food, Refined exposure assessment of polyethylene glycol (E 1521) from its use as a food additive, EFSA J. 16 (6) (2018) e05293.

[2] H.-J. Jang, C.Y. Shin, K.-B. Kim, Safety evaluation of polyethylene glycol (PEG) compounds for cosmetic use, Toxicol. Res. 31 (2) (2015) 105–136.

[3] S. Zalipsky, Chemistry of polyethylene glycol conjugates with biologically active molecules, Adv. Drug Deliv. Rev. 16 (2) (1995) 157–182.

[4] A. Kolate, D. Baradia, S. Patil, I. Vhora, G. Kore, A. Misra, PEG — a versatile conjugating ligand for drugs and drug delivery systems, J. Control. Release 192 (2014) 67–81.

[5] G. Pasut, F.M. Veronese, State of the art in PEGylation: the great versatility achieved after forty years of research, J. Control. Release 161 (2) (2012) 461–472.

[6] A. Arya, A.L. Sharma, Insights into the use of polyethylene oxide in energy storage/conversion devices: a critical review, J. Phys. D 50 (44) (2017) 443002.

[7] S.-L. Chen, R.-H. Fu, S.-F. Liao, S.-P. Liu, S.-Z. Lin, Y.-C. Wang, A PEG-based hydrogel for effective wound care management, Cell Transp. 27 (2) (2018) 275–284.

[8] J.A. DiPalma, P.H. DeRidder, R.C. Orlando, B.E. Kolts, M.B. Cleveland, A randomized, placebo-controlled, multicenter study of the safety and efficacy of a new polyethylene glycol laxative, American Journal of Gastroenterology 95 (2) (2000) 446–450.

[9] E.G. Zurad, J.F. Johanson, Over-the-counter laxative polyethylene glycol 3350: an evidence-based appraisal, Curr. Med. Res. Opin. 27 (7) (2011) 1439–1452.

[10] H.F. Hammer, C.A. Santa Ana, L.R. Schiller, J.S. Fordtran, Studies of osmotic diarrhea induced in normal subjects by ingestion of polyethylene glycol and lactulose, J. Clin. Investig. 84 (4) (1989) 1056–1062.

[11] J. Preston, A.D. Smith, E.J. Schofield, A.V. Chadwick, M.A. Jones, J.E.M. Watts, The effects of Mary Rose conservation treatment on iron oxidation processes and microbial communities contributing to acid production in marine archaeological timbers, PLoS ONE 9 (2) (2014) e84169.

[12] R.M. Seborg, R.B. Inverarity, Preservation of old, waterlogged wood by treatment with polyethylene glycol, Science 136 (3516) (1962) 649.

[13] M.N. Mortensen, H. Egsgaard, S. Hvilsted, Y. Shashoua, J. Glastrup, Characterisation of the polyethylene glycol impregnation of the Swedish warship Vasa and one of the Danish Skuldelev Viking ships, J. Archaeol. Sci. 34 (8) (2007) 1211–1218.

[14] M.N. Mortensen, Stabilization of Polyethylene Glycol in Archaeological Wood, Technical University of Denmark (DTU, Kgs. Lyngby, Denmark, 2009.

[15] J. Glastrup, Y. Shashoua, H. Egsgaard, M.N. Mortensen, Formic and acetic acids in archaeological wood. A comparison between the Vasa Warship, the Bremen Cog, the Oberländer Boat and the Danish Viking Ships, Holzforschung 60 (3) (2006) 259–264.

[16] B. Håfors, The role of the Wasa in the development of the polyethylene glycol preservation method, in: Archaeological Wood, 225, American Chemical Society, 1989, pp. 195–216.

[17] J. Glastrup, Degradation of polyethylene glycol. A study of the reaction mechanism in a model molecule: tetraethylene glycol, Polym. Degrad. Stab. 52 (3) (1996) 217–222.

[18] K.J. Voorhees, S.F. Baugh, D.N. Stevenson, An investigation of the thermal degradation of poly(ethylene glycol), J. Anal. Appl. Pyrol. 30 (1) (1994) 47–57.

[19] M. Bergh, K. Magnusson, J.L. Nilsson, A.T. Karlberg, Formation of formaldehyde and peroxides by air oxidation of high purity polyoxyethylene surfactants, Contact Derm. 39 (1) (1998) 14–20.

[20] J.R. Haines, M. Alexander, Microbial degradation of polyethylene glycols, Appl. Microbiol. 29 (5) (1975) 621.

[21] R. Hamburger, E. Azaz, M. Donbrow, Autoxidation of polyoxyethylenic non-ionic surfactants and of polyethylene glycols, Pharm. Acta. Helv. 50 (1–2) (1975) 10–17.

[22] J.N. Hemenway, T.C. Carvalho, V.M. Rao, Y. Wu, J.K. Levons, A.S. Narang, S.R. Paruchuri, H.J. Stamato, S.A. Varia, Formation of reactive impurities in aqueous and neat polyethylene glycol 400 and effects of antioxidants and oxidation inducers, J. Pharm. Sci. 101 (9) (2012) 3305–3318.

[23] K. Knop, R. Hoogenboom, D. Fischer, U.S. Schubert, Poly(ethylene glycol) in drug delivery: pros and cons as well as potential alternatives, Angew. Chem. Int. Ed. 49 (36) (2010) 6288–6308.

[24] X. Guo, D. Minakata, J. Crittenden, Computer-based first-principles kinetic monte carlo simulation of polyethylene glycol degradation in aqueous phase UV/H2O2 advanced oxidation process, Environ. Sci. Technol. 48 (18) (2014) 10813–10820.

[25] R.S. Goglev, M.B. Neiman, Thermal-oxidative degradation of the simpler polyalkyleneoxides, Polym. Sci. U.S.S.R. 9 (5) (1968) 2351–2364.

[26] L. Chen, S. Kutsuna, S. Yamane, J. Mizukado, ESR spin trapping determination of the hydroperoxide concentration in polyethylene oxide (PEO) in aqueous solution, Polym. Degrad. Stab. 139 (2017) 89–96.

[27] L. Yang, F. Heatley, T.G. Blease, R.I.G. Thompson, A study of the mechanism of the oxidative thermal degradation of poly(ethylene oxide) and poly(propylene oxide) using 1H- and 13C-NMR, Eur. Polym. J. 32 (5) (1996) 535–547.

[28] O.A. Mkhatresh, F. Heatley, A study of the products and mechanism of the thermal oxidative degradation of poly(ethylene oxide) using 1H and 13C 1-D and 2-D NMR, Polym. Int. 53 (9) (2004) 1336–1342.

[29] O.A. Mkhatresh, F. Heatley, A 13C NMR study of the products and mechanism of the thermal oxidative degradation of poly(ethylene oxide), in: Macromolecular Chemistry and Physics, 203, 2002, pp. 2273–2280.

[30] S. Han, C. Kim, D. Kwon, Thermal/oxidative degradation and stabilization of polyethylene glycol, Polymer 38 (2) (1997) 317–323.

[31] J. Glastrup, Stabilisation of polyethylene and polypropylene glycol through inhibition of a β-positioned hydroxyl group relative to an ether group. A study of modified triethylene and tripropylene glycols, Polym. Degrad. Stab. 81 (2) (2003) 273–278.
[32] M.E. Payne, S.M. Grayson, Characterization of synthetic polymers via matrix assisted laser desorption ionization time of flight (MALDI-TOF) mass spectrometry, J. Vis. Exp. (136) (2018) e57174, doi:10.3791/57174(2018).
[33] C. Wesdemiotis, N. Solak, M.J. Polce, D.E. Dabney, K. Chaicharoen, B.C. Katzenmeyer, Fragmentation pathways of polymer ions, Mass. Spectrom. Rev. 30 (4) (2011) 523–559.
[34] J. Ulbricht, R. Jordan, R. Luxenhofer, On the biodegradability of polyethylene glycol, polypeptoids and poly(2-oxazoline)s, Biomaterials 35 (17) (2014) 4848–4861.
[35] J.A. Giroto, A.C.S.C. Teixeira, C.A.O. Nascimento, R. Guardani, Degradation of poly(ethylene glycol) in aqueous solution by photo-fenton and H2O2/UV processes, Ind. Eng. Chem. Res. 49 (7) (2010) 3200–3206.
[36] C.W. McGary Jr, Degradation of poly(ethylene oxide), J. Polym. Sci. 46 (147) (1960) 51–57.